

## RESEARCH ARTICLE

# Small-scale production of synthetic natural gas by allothermal biomass gasification

Alexander Tremel<sup>\*,†</sup>, Matthias Gaderer and Hartmut Spliethoff

Institute for Energy Systems, Technische Universität München, Boltzmannstraße 15, 85748 Garching, Germany

## ABSTRACT

The gasification of biomass can be coupled to a downstream methanation process that produces synthetic natural gas (SNG). This enables the distribution of bioenergy in the existing natural gas grid. A process model is developed for the small-scale production of SNG with the use of the software package AspenPlus (Aspen Technology, Inc., Burlington, MA, USA). The gasification is based on an indirect gasifier with a thermal input of 500 kW. The gasification system consists of a fluidized bed reformer and a fluidized bed combustor that are interconnected via heat pipes. The subsequent methanation is modeled by a fluidized bed reactor. Different stages of process integration between the endothermic gasification and exothermic combustion and methanation are considered. With increasing process integration, the conversion efficiency from biomass to SNG increases. A conversion efficiency from biomass to SNG of 73.9% on a lower heating value basis is feasible with the best integrated system. The SNG produced in the simulation meets the quality requirements for injection into the natural gas grid. Copyright © 2012 John Wiley & Sons, Ltd.

## KEY WORDS

biomass gasification; synthetic natural gas; substitute natural gas; SNG; process simulation; small scale

## Correspondence

\*Alexander Tremel, Institute for Energy Systems, Technische Universität München, Boltzmannstraße 15, 85748 Garching, Germany.

†E-mail: tremel@tum.de

Received 15 December 2011; Revised 7 April 2012; Accepted 8 April 2012

## 1. INTRODUCTION

Using biomass is an option that lowers the dependency on fossil fuels such as natural gas and thus reduces CO<sub>2</sub> emissions. Because of the low specific energy density of biomass, it should be utilized in a distributed system to minimize transportation efforts. The European Union (EU) endorses a binding target of a 20% share of renewable energies in the total primary energy consumption in 2020. Furthermore, the EU members are aiming for a 10% share of biofuels in overall EU transport petrol and diesel consumption in the same time frame [1]. The distributed production of SNG from biomass can contribute to the performance of both obligations.

Today, biomass power plants produce electricity in a power range typically up to 20 MW<sub>e</sub> with electrical efficiencies of 30%. With an optimized biomass system, heat is also produced. To maintain high system efficiency, it is useful to have an appropriate heat consumer such as a heat grid or industry process that is capable of using a constant heat flux of approximately 20–40 MW. This requirement limits the possible locations for a combined heat and power plant. On the other hand, downscaling of

the plant causes lower electrical efficiencies and higher specific investment costs.

Along with the electricity grid, the natural gas grid can also be used for energy distribution. Biomass can be converted to synthetic natural gas (SNG) and supplied to the existing natural gas grid. The conversion efficiency of such a process can be up to 74% based on the lower heating value (LHV) for multi-megawatt processes [2]. Heat might be still released but in lower quantities than for electricity production. As the heat release from the methanation is rather at a high temperature, it can be used for power production (steam cycle or organic Rankine cycle) if the scale is large enough. Compared with the conventional combined heat and power production (CHP) from biomass, it is easier to find an appropriate heat consumer for these smaller quantities. Furthermore, the process could be economically competitive without the usage of the heat release. Bioenergy in the form of SNG can be stored using the fully developed natural gas storage technique. The gas grid itself can compensate small fluctuations between SNG production and utilization, and SNG can be stored in existing natural gas storage facilities.

The distributed SNG production offers several possibilities for further utilization. It can be used for subsequent electricity production, for heat production, as a transportation fuel, and for domestic heating and cooking systems. Furthermore, it decreases the dependency on imported natural gas.

Biochemical fermentation can be seen as a competitive process to SNG generation. But fermentation mainly uses specific crop sources and thus competes with food production. For instance, in Germany, the thermo-chemical potential achieved by biomass gasification is more than three times larger than the biochemical potential of fermentation [3]. The first process step of SNG generation from biomass is a thermo-chemical gasification, which enables the use of different kinds of biomass and residuals that are not in competition with the food chain.

The target plant size for SNG production is usually in the multi-megawatt range, and the process simulations found in literature focus on the SNG production on a large scale. Marechal *et al.* presented a process design for the generation of SNG [4] and published a techno-economic analysis for a biomass input of 20 MW [5]. The Energy Research Centre of the Netherlands developed an integrated SNG system [6] and later presented a detailed process simulation to calculate the process efficiency for a biomass input of 1 GW based on three different types of gasifiers [7]. At Chalmers University of Technology, Heyne *et al.* studied the integration of fixed bed and fluidized bed methanation in an SNG production process for a biomass input of 100 MW [8,9]. Furthermore, they investigated the integration of SNG production with an existing combined heat and power unit that has a size of 100-MW fuel input [10]. Jurascik *et al.* focused on the exergy analysis of biomass to SNG conversion [11,12] and analyzed a target process size of 180 MW. Rehling *et al.* [13] developed a simulation tool for the overall SNG process based on the Repotec gasifier in Güssing (Austria). They first modeled the SNG production from a side stream of the gasifier and then modeled a gasification unit and a corresponding SNG unit with a biomass input of 10 MW. The potential of fluidized bed methanation using this configuration is shown by experimental results from a 1-MW reactor [14].

The large commercial interest of the SNG production from biomass is shown by current activities in this field. In Sweden, the GoBiGas project aims at the installation of a 20-MW demonstration plant in 2013 and the subsequent design of an 80- to 100-MW plant [15]. The Bio2G project aims at an SNG production of 200 MW, and the planned start of construction is in 2013 [16].

The target plant size of centralized SNG production is  $10 \text{ MW}_{\text{th}}$  to  $1 \text{ GW}_{\text{th}}$ , which requires usually large biomass transportation volumes, may have negative environmental impacts, and requires an appropriate heat consumer. In contrast, SNG production in small distributed systems is a way of minimizing the local environmental impact and finding an appropriate heat consumer. Because installations on a larger scale are usually advantageous in

efficiency (less specific losses and better options for heat integration) and specific costs (economy of scale), both large-scale and small-scale systems could complement each other. The optimum scale of an SNG production unit depends on site-specific issues and cannot be generally stated. A requirement for the location of the facility in all cases is the access to the gas grid that limits the number of sites.

The advantages and the economic potential of small-scale biomass gasification plants have already been shown for electricity production [17], but the application of biomass gasification for SNG production is not considered yet. A small-scale SNG process can be based on indirect steam gasification via the Biomass Heat Pipe Reformer (BioHPR) [18–20]. The first commercial facility of this kind with a thermal input of 500 kW has been installed near Munich, Germany.

The objective of the simulation approach presented here is evaluation of a small-scale SNG production based on the BioHPR. The model parameters of the simulation are adjusted to the operation experience of the small-scale gasifier and cannot be directly compared with larger-scale plants.

An important part of the modeling is the simulation of the reactions within the gasifier. The complexity of a model approach for fluidized bed gasification depends on the application and reaches from the design of complete industrial processes to the complex simulation of a unit [21]. An overview of different approaches for the modeling of biomass gasification is given by Puig-Arnavat *et al.* [22], Buragohain *et al.* [23], and Abuadala and Dincer [24].

Although the chemical equilibrium is usually not approached at the operating conditions of a fluidized bed, the assumption of chemical equilibrium is usually used in flowsheet simulations of biomass gasification [7,12,25–29]. As the kinetics of biomass gasification are dependent on the specific operating conditions and the specific fuel properties, gasification kinetics usually are not considered in flowsheet simulations.

For the simulation presented in this paper, a chemical equilibrium approach is extended using experimental data, and a good correlation of the model and the measurements is found at different operating conditions.

## 2. PROCESS LAYOUT

The production route of SNG from biomass that is considered here consists of four process units that are shown in Figure 1. In the first step, biomass is gasified to synthesis gas in an endothermic reaction. Then, a gas cleaning stage is needed to prevent the methanation catalyst from poisoning. In the catalytic methanation process (highly exothermic), the synthesis gas is converted to methane-rich gas with the by-products  $\text{CO}_2$  and water steam. These two by-products are removed in a gas

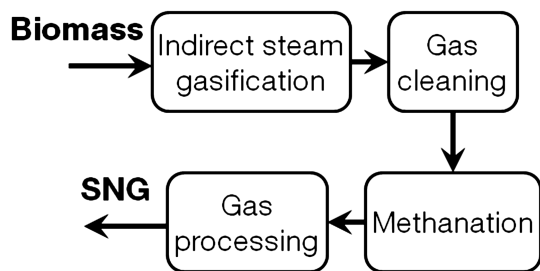


**Figure 1.** The four basic process steps of synthetic natural gas (SNG) production.

processing unit in order to increase the LHV and meet the requirements for injecting the SNG into the natural gas grid.

### 2.1. Gasification

In the work presented here, the BioHPR is used for the gasification step. The system consists of two fluidized beds, combustor and reformer, that are interconnected via heat pipes. In the lower bed, biomass is burned with air in an exothermic reaction. The heat released in the combustor is transported via heat pipes to the reformer. This second bed is fluidized by steam, and biomass is converted to synthesis gas in endothermic gasification reactions. The heat pipes use sodium as the working fluid. Liquid sodium is evaporated in the combustion fluidized bed, and the sodium vapor rises to the reformer. As heat is released during the condensation of sodium vapor, heat can be transferred almost isothermally from the combustion fluidized bed to the reformer.

Char that is produced in the gasification zone can be fed to the combustor. Char is transported together with small amounts of bed material via a siphon duct that allows the operation of the reformer at an increased pressure. For further information about the BioHPR, please see [18,20]. The BioHPR could be replaced by any other allothermal biomass gasifier that is designed for a small-scale process ( $<1 \text{ MW}_{\text{th}}$ ). The gasifier is operated with spruce wood, and the fuel properties are given in Table I.

Because of the indirect steam-blown gasification, a hydrogen, methane-rich, and almost nitrogen-free synthesis gas is produced. A high hydrogen partial pressure is favorable for the methanation reaction [30]. A high initial yield of methane is attractive because the conversion of hydrogen and CO to methane in the methanation reactor involves approximately 20% efficiency loss due to heat

production [6]. A nitrogen fraction would dilute the SNG produced. The synthesis gas quality favors an indirect gasification process for SNG production when compared with a high-temperature entrained-flow gasifier and an oxygen-blown circulating fluidized bed [6]. An indirect gasification process can be operated without the need of an air separation unit. Furthermore, the carbon conversion is expected to be higher because the final burn-off occurs in a combustion environment in the combustion fluidized bed [6].

The reformer of the BioHPR is operated at elevated pressure (0.4 MPa), which favors the conversion to methane in the subsequent methanation reactor [31] that is operated at the same pressure level. An intermediate compression after the gasification is not required.

### 2.2. Synthesis gas cleaning

In addition to the main gas fractions ( $\text{H}_2$ ,  $\text{H}_2\text{O}$ ,  $\text{CO}$ ,  $\text{CO}_2$ , and  $\text{CH}_4$ ), the synthesis gas contains undesirable gas components (i.e., sulfur and chlorine components), tars, and dust particles. For particle removal, a combination of cyclone and ceramic cartridge filters can be used [18,32]. Tar compounds can be removed at low temperature with water and organic scrubbers or at high temperature with a catalytic converter. A water scrubber leads to a condensation of steam from the synthesis gas that has to be re-added to the gas stream in order to prevent carbon formation within the methanation reactor. In contrast, an organic scrubber (e.g., [33]) is advantageous as it is operated above the steam condensation temperature. Alternatively, catalytic reforming converts tars to smaller compounds via a cracking reaction and might increase the caloric value of the gas. The temperature range required for tar reforming is between 750 and 900 °C [34]. Recent developments (e.g., [35–37]) suggest that the application of catalytic tar reforming is suitable for a small-scale biomass gasification process. As a negative effect, tar reforming is likely to reduce the  $\text{CH}_4$  content of the synthesis gas as  $\text{CH}_4$  is converted at the catalyst. This would lower the overall biomass to SNG efficiency.

However, it is possible that tar removal is not required for the SNG process if the temperature of the synthesis gas never falls below the tar condensation temperature. In this case, tars entering the methanation reactor can be converted at the methanation catalyst. Recent investigations demonstrated the ability to reform light tars when the water gas shift reaction and the methanation reactions take place in a fluidized bed reactor [38]. However, carbon formation that reduces the performance of the catalyst is possible, and there is the need for further research in this field.

Gaseous halide compounds (mainly HCl) and sulfur compounds (mainly  $\text{H}_2\text{S}$  and COS) result in a deactivation of the methanation catalyst and therefore have to be removed. For small-scale processes, a suitable gas cleaning process is dry adsorption in fixed beds. Halides can be removed with  $\text{Na}_2\text{CO}_3 \cdot \text{NaHCO}_3 \cdot 2\text{H}_2\text{O}$  at an operation temperature around 400 °C [39].

**Table I.** Elemental composition (dry ash free) of spruce wood used in the simulation (ash content 0.6 wt% on a dry basis, moisture content 25 wt%).

Element	C	H	O	N
% (weight) dry ash free	49.8	6.3	43.2	0.13

Sulfur removal can be done with a ZnO-fixed bed at around 400 °C and has the potential to decrease the sulfur concentration below the limit for methanation [40] (i.e., 1 ppm [41]).

### 2.3. Methanation

The methanation of synthesis gas from coal gasification is a well-developed process. Much research was done in the USA in the early 1970s because of the oil shortage. In the 1980s, most of the research was stopped because of the low oil prices, but a 900-MW SNG plant was constructed in North Dakota in 1984, and it is still in operation [42].

The principal reactions within the methanation process are shown in Table II [31].

The enthalpies of reactions were calculated using the FactSage software package [43] at 300 °C, a typical methanation temperature.

For operation of the methanation process, it is essential to avoid both reaction (R4) and the reverse of reaction (R5) because carbon formation would deactivate the catalyst. In the methanation reactor, carbon formation is mainly dependent on the steam-to-biomass ratio SB and the temperature. SB is the mass flow of water related to dry ash-free (daf) biomass within the system. The water mass flow consists of moisture from biomass, steam added to the gasifier, and steam added during the methanation.

Biomass (defined for the simulation as dry ash free, or daf) is first converted to synthesis gas in the gasifier and then fed to the methanation reactor. The probability of carbon formation during methanation can be evaluated by considering the chemical equilibrium at operation condition of the methanation reactor. Carbon is thermodynamically stable below the lines (dependent on pressure) in Figure 2. The calculations were performed with the FactSage software package [43].

On a small scale, the feedstock is expected to vary significantly between different SNG plants, but woody biomass is expected to be a potential fuel. Therefore, source spruce wood is chosen as a representative biomass, and its elemental composition is given in Table I. Other elements and ash are not considered in the equilibrium calculation because these components are removed prior to methanation. Steam is added before entering the methanation reactor if the SB is below the carbon formation boundary to prevent a deactivation of the catalyst.

**Table II.** Basic reactions within the methanation process (enthalpies of reaction calculated at 300 °C by using the FactSage software package).

$\text{CO} + 3 \text{H}_2$	$\leftrightarrow$	$\text{CH}_4 + \text{H}_2\text{O}$	$\Delta H_{\text{R}} = -217.1 \text{ kJ/mol}$	(R1)
$\text{CO} + \text{H}_2\text{O}$	$\leftrightarrow$	$\text{H}_2 + \text{CO}_2$	$\Delta H_{\text{R}} = -39.2 \text{ kJ/mol}$	(R2)
$\text{CO}_2 + 4 \text{H}_2$	$\leftrightarrow$	$\text{CH}_4 + 2 \text{H}_2\text{O}$	$\Delta H_{\text{R}} = -177.9 \text{ kJ/mol}$	(R3)
$2 \text{CO}$	$\leftrightarrow$	$\text{C} + \text{CO}_2$	$\Delta H_{\text{R}} = -173.6 \text{ kJ/mol}$	(R4)
$2 \text{H}_2 + \text{C}$	$\leftrightarrow$	$\text{CH}_4$	$\Delta H_{\text{R}} = -82.7 \text{ kJ/mol}$	(R5)

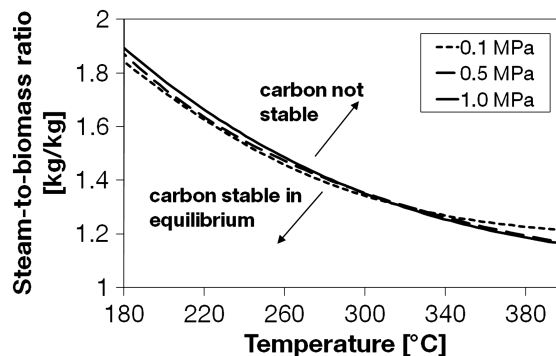


**Figure 2.** Carbon formation potential during methanation as a function of temperature, steam-to-biomass ratio, and total pressure.

Both the reactions of CO (R1) and CO<sub>2</sub> (R3) to methane are highly exothermic. Such high heats of reaction cannot be absorbed by the process stream in an adiabatic reactor unless the CO and CO<sub>2</sub> conversion is limited to less than about 2.5 moles per 100 moles of feed gas [31]. As CO and CO<sub>2</sub> concentrations are typically in the range of 10–20% (mole fraction) in an indirect steam gasifier, the cooling of the methanation zone is essential.

A low reaction temperature and a high reaction pressure shift the methanation equilibrium towards methane. The methane yield is defined as the mass flow of methane related to the mass flow of biomass (daf) entering the system. The methane yield as a function of reaction temperature and pressure is calculated in the case of chemical equilibrium and shown in Figure 3.

With increasing pressure, the pressure effect decreases. An increase from atmospheric pressure to 0.5 MPa has approximately the same influence on the methane yield as it further increase to 2 MPa. The methanation benefits from slightly increased pressures; higher pressures are not required. If no intermediate compression between gasifier and methanation reactor is used, the methanation reaction benefits from an elevated gasification pressure.

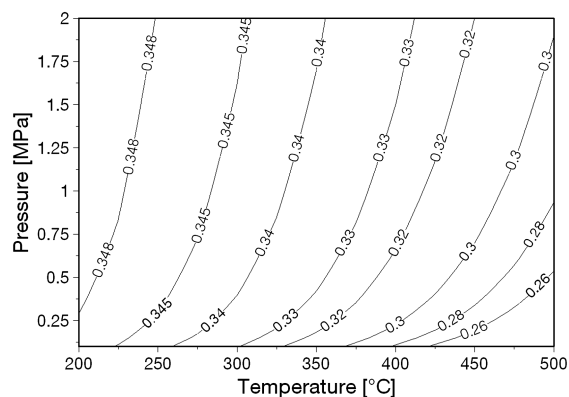


**Figure 3.** Methane yield from biomass (dry ash free) considering chemical equilibrium (steam-to-biomass ratio 2).



The combination of fluidized bed and heat pipes that has been developed for the BioHPR can be adapted to the methanation reactor. The methanation catalyst is used as the bed material. This setup enables a homogeneous temperature distribution within the reactor and prevents the occurrence of hot spots during the exothermic reaction. A recent study [44] shows that the catalyst fluidization results in a reduced tendency towards carbon deposition and subsequent deactivation. The heat pipes that remove heat from the reaction zone can be operated with water as the working fluid. For a methanation temperature of around 300 °C, a typical heat pipe working temperature is 250 °C. This corresponds to an internal heat pipe pressure of 4.0 MPa, which can be handled with steel tubes. The heat pipes are back cooled in a pressurized boiler at, for example, 1.0 MPa and 180 °C. With this system, the reaction heat of the methanation is used to produce pressurized steam.

In a fluidized bed, abrasion and loss of the catalyst may occur. This would require the continuous or batch-wise addition of catalyst and could decrease the economic performance. An evaluation of this effect is not possible at this stage of development. As the operation of fluidized bed methanation is proven on a larger scale (e.g., Thyssengas Comflux process [45]), the fluidized bed methanation reactor seems to be a promising technology.

#### 2.4. Gas processing

After methanation, the raw SNG consists mainly of methane, water steam, and CO<sub>2</sub>. Before SNG is fed to the natural gas grid, gas processing is required to remove H<sub>2</sub>O and CO<sub>2</sub>. The H<sub>2</sub>O content of the raw SNG can be up to 60% by volume [6]. H<sub>2</sub>O removal is achieved by condensation, adsorption, and absorption. For a small-scale process, a combination of condensation at ambient temperature and an adsorption process seems to be economically reasonable.

CO<sub>2</sub> is removed by pressure swing adsorption (PSA), pressurized water scrubbers, amine scrubbers, membrane systems, or cryogen units. A small-scale process can be equipped with a PSA that is operated at approximately 0.8 MPa [3]. Finally, SNG is compressed to grid pressure and fed to the natural gas grid.

### 3. PROCESS SIMULATION

The overall process is simulated using the AspenPlus software package (version 2006.5; Aspen Technology, Inc., Burlington, MA, USA), a modeling tool performing rigorous material and energy balance calculations. User-defined subroutines can be implemented into the simulation by using FORTRAN codes. The input parameters for the simulation are summarized in Table III.

The simulation is performed on the basis of mass and energy balances, but the detailed design or engineering of components (for example, heat exchangers), material selection, and corrosion issues are not considered.

#### 3.1. Gasification

The simulation flowsheet for the gasification part is shown in Figure 4. Spruce wood (moisture content = 25%; LHV (wet basis) = 14.55 MJ/kg; elemental composition, see Table I) is used as the fuel. The low moisture content is required to store the wood chips and avoid deterioration and self-heating. The wood chips are fed to the gasifier by a lock hopper system that requires 1.8 Nm<sup>3</sup>/h fresh air. Compressed air for biomass feeding is used because it is available on site. Actuators and valves of the BioHPR are operated with compressed air. Therefore, the use of air for the lock hopper is the simplest solution and is currently used. The feeding of O<sub>2</sub> and N<sub>2</sub> to the reformer is considered in the simulation and also in the determination of the gasification model.

The pyrolysis is simulated by an Aspen RYield block that decomposes the feed into its simple components carbon, oxygen, hydrogen, nitrogen, sulfur, chlorine, and ash according to the biomass ultimate analysis. Ash and part of the feed carbon can leave the reformer after the pyrolysis forming char that is fed to the combustor (COMB). The other components are fed to the gasification block (GAS) that is simulated by an Aspen RGibbs reactor. Steam is used as fluidization and gasification agent and enters the gasification block at a constant temperature of 600 °C. The steam-to-biomass ratio SB is defined as mass flows of steam and biomass moisture relative to the mass flow of biomass (daf) reduced by the char mass flow that is fed to the combustor. This char mass flow rate is dependent on the fuel properties and process conditions and is about 11–13% of the initial biomass feed rate (dry basis).

$$SB = \frac{\dot{m}_{\text{H}_2\text{O}}}{\dot{m}_{\text{Biomass,daf}}} = \frac{\dot{m}_{\text{Steam}} + \dot{m}_{\text{Moisture}}}{\dot{m}_{\text{Feed,daf}} - \dot{m}_{\text{Char}}} \quad (1)$$

A chemical equilibrium calculation predicts a minimum value for SB of approximately 0.3 in order to achieve a complete gasification of biomass at a temperature of 700 °C. To achieve good fluidization of the reformer, a constant SB of 0.6 is assumed. This value is within the lower range of SB ratios realized with a 150-kW test facility [18].

The gasification model is based on the principle of the minimization of the Gibbs free energy. In the simulation, a constant gasifier exit temperature of 700 °C, which corresponds to experiments at the test facility, is used. In order to adjust the gas composition of the synthesis gas to experimental data, a restricted chemical equilibrium method is defined. The chemical equilibrium can be adjusted to a defined temperature that deviates from the real gas temperature. The difference between the two temperatures is called restricted equilibrium temperature (RET).

Several experimental datasets [18] that provide dry synthesis gas composition for different values of biomass and steam mass flows are available. For each dataset, the optimum RET is evaluated by an AspenPlus simulation

**Table III.** Summary of the simulation input parameters.

Thermal biomass input		500 kW
Temperatures	Ambient (fuel, air, and water)	25 °C
	Reformer steam in	600 °C
	Reformer outlet	700 °C
	Reformer RET	115 °C
	Combustor outlet	900 °C
	Air preheater outlet	750 °C
	Flue gas exit	140 °C
	Synthesis gas cleaning	400 °C
	Methanation	270 °C
	PSA inlet	30 °C
Heat losses	Reformer	3 kW
	Combustor	3 kW
	Methanation reactor	3 kW
	Cooling during gas cleaning	50 °C
Pressures	Ambient (fuel, air, and water)	0.1 MPa
	Reformer	0.4 MPa
	Steam generator	0.7 MPa
	Combustion air compressor outlet	0.12 MPa
	Flue gas recycle blower outlet	0.12 MPa
	Steam boiler for heat pipe cooling (methanation)	1.0 MPa
	PSA	0.6 MPa
Pressure drops	Reformer	0.02 MPa
	Combustor	0.025 MPa
	Synthesis gas cleaning	0.02 MPa
	Methanation reactor	0.02 MPa
Air to fuel ratio $\lambda$ (lambda)	Combustor	1.2
Steam to biomass ratio	Reformer	0.6
SNG upgrading	CO <sub>2</sub> removal	96%
	CH <sub>4</sub> loss	2%
Pump/compressor efficiency	isentropic	0.6
	mechanical	0.9

RET, restricted equilibrium temperature ; PSA, pressure swing adsorption; SNG, synthetic natural gas.

for the given mass flows. The relationship between the optimum RET for a given dataset and the experimental SB is shown in Figure 5. For higher SB, an increasing RET is required to fit the experimental gas composition. The trend of the data can be described using a least square fitting procedure and a linear approximation.

However, using positive RETs leads to chemical equilibrium compositions at temperatures higher than 700 °C and consequently to an underestimation of the methane content. This is compensated for by producing CH<sub>4</sub> in an external RYield block (CH<sub>4</sub>-Generator). The methane content is adjusted to the real gas concentration of each experiment of the dataset. An exact fit of the measured and predicted CH<sub>4</sub> concentrations is achieved by converting a percentage of carbon directly to methane. In the simulation, the average percentage of all calculations is then used, that is, always 20% of the initial carbon from biomass is converted to methane.

The heat of reaction of the CH<sub>4</sub> production as well as of the pyrolysis reactions are integrated in the gasification block (GAS). In the simulation, the heat requirements of the overall gasification process (including pyrolysis and CH<sub>4</sub> production) are balanced by the heat supply of the heat pipes.

The simulated dry synthesis gas compositions compared with the experimental gas composition of two datasets are shown in Table IV.

Char that is separated after the pyrolysis is fed to the combustor (COMB). Additional biomass can also be fed directly to the combustor if more heat is required. The flue gas leaves the combustor at a temperature of 900 °C and passes an air preheater. The residual heat of the flue gas is used to produce steam in a flue gas boiler. Cold flue gas is recycled to the combustor in order to adjust the amounts of combustion heat discharged by heat pipes and flue gas boiler. The variation of the recirculation rate directly influences the heat balance. A higher recycle rate increases the mass flow through the

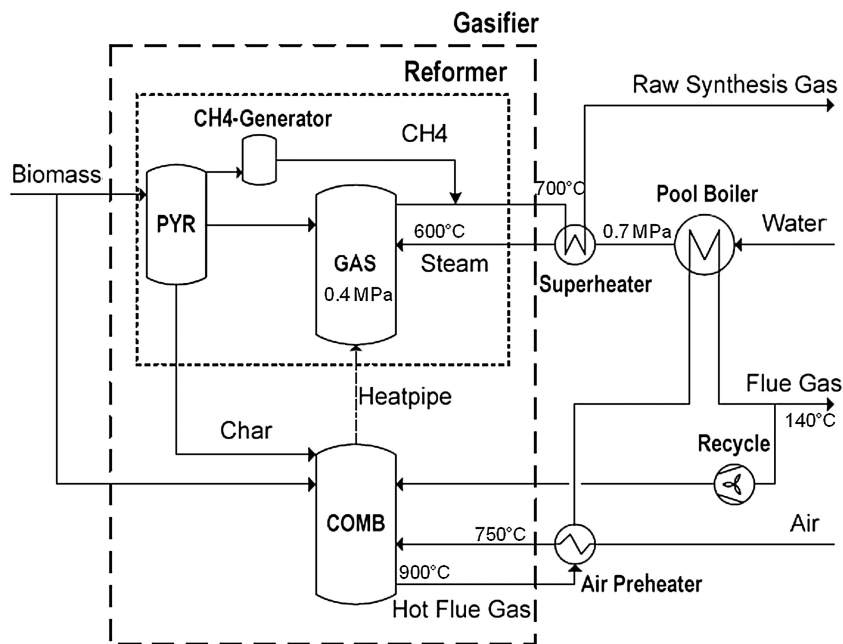


Figure 4. Simulation flowsheet of the gasification unit.

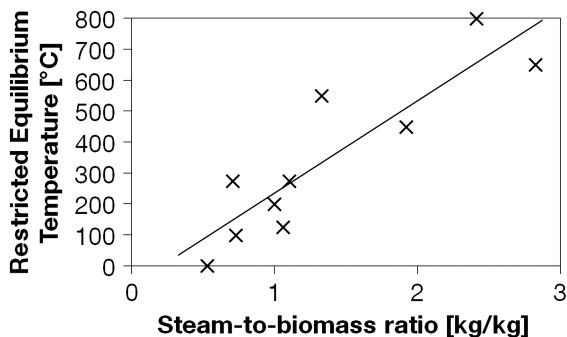


Figure 5. Restricted equilibrium temperature as a function of the steam-to-biomass ratio. Crosses (X) denote experimental data.

combustion fluidized bed. This leads to more heat being shifted to the flue gas boiler.

### 3.2. Synthesis gas cleaning

The process flowsheet of gas cleaning, methanation, and gas processing units is shown in Figure 6. The raw

synthesis gas is first cooled with water steam to the gas cleaning inlet temperature of 450 °C. Sulfur and chlorine compounds are removed by dry adsorption in two fixed beds that are simulated by separators. Heat losses result in a temperature drop of 50 °C.

The dry adsorption methods are used as the product gas after the gasification of wood contains low amounts of chlorine and sulfur components.

During the current operation of the BioHPR with a hot gas clean-up and a subsequent gas turbine, a major condensation of tars is not detected. Therefore, the transfer of tars to the methanation reactor is expected, and a tar removal stage is not included because of the possibility of tar conversion at the methanation catalyst.

### 3.3. Methanation

Before entering the methanation, reactor steam is added to the clean synthesis gas in order to avoid carbon formation at the catalyst. The fluidized bed methanation reactor is simulated by an RGibbs reactor at the

Table IV. Simulated gas composition (dry basis) of the gasifier model compared to experimental data.

Gas composition (dry) [% (mole fraction)]	Dataset 1 (SB = 0.53)		Dataset 2 (SB = 0.73)	
	Experiment	Simulation (RET = 94 °C)	Experiment	Simulation (RET = 154 °C)
H <sub>2</sub>	39.8	39.7	40.8	40.7
CO	23.5	27.2	23.5	24.2
CO <sub>2</sub>	19.4	15.5	20.4	17.4
CH <sub>4</sub>	10.2	10.1	9.2	9.7
N <sub>2</sub>	7.1	7.4	7.1	8.0

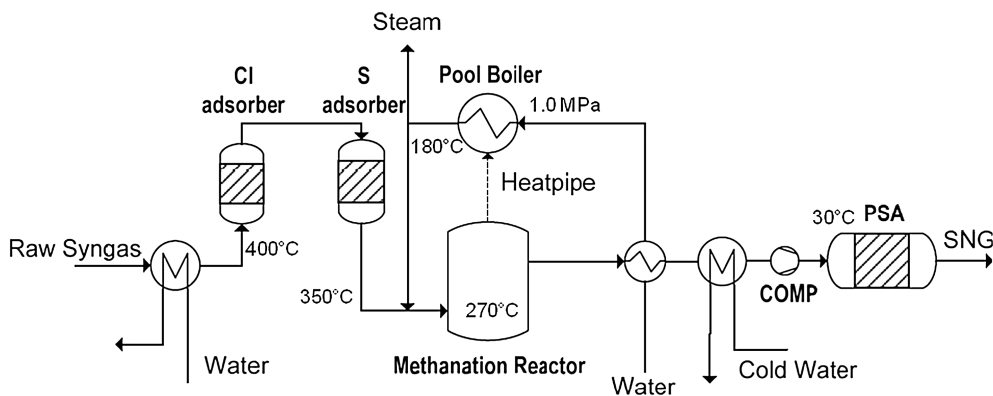


Figure 6. Simulation flowsheet of gas cleaning, methanation, and gas processing.

isothermal reactor temperature of 270 °C. In literature, the reaction temperature of fluidized bed methanation varies between 200 and 500 °C [45]. As the chemical equilibrium favors the generation of methane at lower temperature, a temperature at the lower end (270 °C) is chosen in the simulation. However, as the reaction kinetics are favored at a higher temperature, the low temperature might increase the reaction time and might require larger reactor geometry.

As the methanation reactions are highly exothermic, the reactor is cooled by heat pipes that transport the heat to a pressurized boiler. The temperature difference along the heat pipes is set to 90 °C to enable a sufficient heat transfer. Water steam is produced at a pressure of 1.0 MPa and at a corresponding temperature of 180 °C.

The water fed to the boiler is preheated by the raw SNG. The saturated steam leaving the boiler is partly used to increase the SB prior to methanation. The excess steam leaves the process and can be used externally.

### 3.4. Gas processing

The first gas processing step is a cooling to 60 °C in order to condense most of the steam. Then, cold water at a temperature of 3 °C is used to further reduce the water content of the gas. A PSA process at 0.8 MPa removes 96% of CO<sub>2</sub> from the SNG. The operating conditions of the PSA are taken from a technical review of existing gas upgrading technologies [46]. The gas processing causes a methane loss of 2%. To avoid a release of methane to the atmosphere, the off-gas of the PSA should be treated in a catalytic converter. This additional treatment is not considered in the process simulation.

The compression to grid pressure is not considered in the simulation because the pressure range is dependent on the point of injection.

## 4. PROCESS INTEGRATION

The heat integration of a small-scale process is limited by the number and interconnection of heat exchangers. The

need for the compactness of the system limits the possibilities for heat integration. For example, the off-gas of each fluidized bed has to be used to heat the inlet gas stream to the fluidized bed to enable a compact design. Therefore, steam is superheated to 600 °C by cooling the product gas of the reformer. The combustion air is preheated by the exhaust gas of the combustor.

As the number of metering points (for gas concentration, temperature, pressure, etc.) is limited for a small-scale system because of cost issues, a leakage within a heat exchanger is not readily detected. Therefore, the formation of an explosive atmosphere (for example, by mixing air with gasifier product gas) has to be prevented by the assembly of the heat exchangers.

Because of the limitations that arise from the small scale of the system, a general methodology (for example, Pinch analysis) is not applied. The process integration is studied by the definition of different cases.

The main process steps of synthesis gas production are the conversion of biomass to synthesis gas and the methanation. The production of synthesis gas is an endothermic process. The heat required for conversion is delivered by an exothermic combustion in a separate fluidized bed. An integration of the two reactors is possible by feeding char that is produced during pyrolysis in the reformer to the combustion reactor. If more heat is required, biomass can also be fed directly to the combustion reactor. The firing of biomass to the combustion reactor instead of dry char leads to efficiency losses, and an integration of reformer and combustion reactor is to be preferred.

As steam production for indirect steam gasification requires large amounts of heat and the methanation of synthesis gas is highly exothermic, there is the possibility of integrating the two processes. During normal BioHPR operation, the steam required for indirect gasification is produced in a boiler. This boiler is heated by flue gas from the combustion reactor that is again fed by char or biomass.

Heat integration is possible by using steam produced from cooling the methanation reactor. In that case, less char and biomass need to be fed to the combustion reactor,



which again increases the conversion efficiency. However, the flue gas boiler is still required for system start-up because the gasifier has to be operated prior to the methanation reactor.

Flowsheet simulations, that show different system integrations and outline the potential of the overall process, are performed. With either the gasification process and/or the methanation integrated, four process operation modes are possible.

#### Process 1 (non-integrated system)

With biomass fed to the reformer and to the combustor, the gasification is easy to control. Steam for the indirect gasification is produced in a boiler that is heated by flue gas from the combustion reactor. The flue gas recycle rate is adjusted to the needs of the heat flux of heat pipes and flue gas boiler. With the recirculation rate increased, the theoretical adiabatic combustion temperature in the fluidized bed is decreased and less heat can be transferred by the heat pipes. Consequently, as the outlet temperature of the fluidized bed remains constant, heat is shifted to flue gas boiler and more steam can be produced.

The methanation is operated independently. As char has to be converted completely in the reformer, the required fuel residence time in the reformation zone is high.

#### Process 2 (char integration)

A modification of the process is the integration of reformer and combustor. Char that is generated during pyrolysis in the reformer is fed to the combustor. The amount of char that enters the combustion reactor is specified by a calculation of heat required for the heat pipes and the flue gas boiler.

It is assumed that the fixed carbon fraction of the biomass is sufficient for the char requirement. Because of the integration, the fuel residence time in the reformer can be shorter.

The feeding of char to the combustion zone is a standard option in prior art two-stage fluidized bed gasifiers.

#### Process 3 (steam integration)

Another possible integration is the link between reformer and methanation reactor. Steam is produced by cooling the methanation reactor and is fed to the reformer. The combustor is exclusively fed by biomass.

#### Process 4 (char and steam integration)

The fully integrated system combines the two options for integration. The combustor is only fed by char from the reformer, and the steam required for indirect gasification is produced by cooling the methanation reactor.

## 5. RESULTS AND DISCUSSION

### 5.1. Process performance

In order to evaluate the benefits from process integration and to compare the four processes, different efficiencies are defined. The conversion efficiency  $\eta_C$  relates the chemical enthalpy of the SNG to the thermal biomass input on an LHV (wet) basis.

$$\eta_C = \frac{\dot{m}_{\text{SNG}} \cdot \text{LHV}_{\text{SNG}}}{\dot{m}_{\text{Biomass}} \cdot \text{LHV}_{\text{Biomass}}} \quad (2)$$

The net efficiency  $\eta_{\text{net}}$  considers the auxiliary electricity consumption of the process:

$$\eta_{\text{net}} = \frac{\dot{m}_{\text{SNG}} \cdot \text{LHV}_{\text{SNG}} - P_{\text{el}}/\eta_{\text{ref}}}{\dot{m}_{\text{Biomass}} \cdot \text{LHV}_{\text{Biomass}}} \quad (3)$$

The overall efficiency  $\eta_{\text{overall}}$  includes the heat released in different process units as a product:

$$\eta_{\text{overall}} = \frac{\dot{m}_{\text{SNG}} \cdot \text{LHV}_{\text{SNG}} + \dot{Q} - P_{\text{el}}/\eta_{\text{ref}}}{\dot{m}_{\text{Biomass}} \cdot \text{LHV}_{\text{Biomass}}} \quad (4)$$

The reference efficiency for power production  $\eta_{\text{ref}}$  is set to 0.4. To enable realistic heat utilization, all heat sources down to a minimum temperature of 60 °C are considered because this is a common water return temperature from a standard heat grid. The heat that is released below 60 °C is neglected.

The efficiencies obtained with the different processes are summarized in Figure 7. The energy balance (biomass input, SNG output, auxiliary power demand, and heat output) is given in Table V.

The conversion efficiency of process 1 is 66.8%. It can be increased by 4.6 percent points by using char integration and by 0.1 percent points by using steam integration, respectively. When both options are integrated, a conversion efficiency of 73.7% is technically feasible. The net efficiency is, in all cases, approximately 5 percent points lower because of the electrical consumption of the system that is always in the range of 10 kW<sub>e</sub>. The inclusion

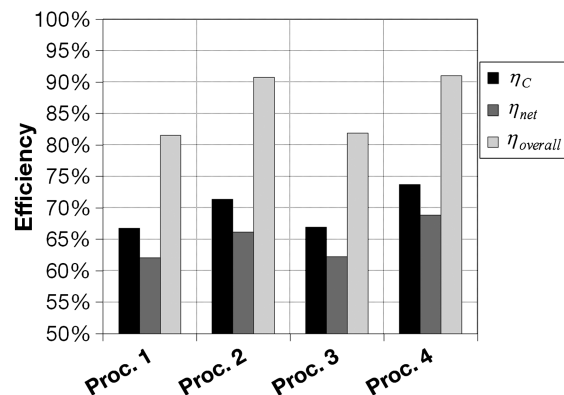


Figure 7. Process efficiency for different levels of process integration.

**Table V.** Energy and feed balance for different process integration options.

Process no.	1	2	3	4
Biomass input (kW)	500	500	500	500
Biomass fraction to reformer (%)	70.2	100	71.1	100
Biomass fraction to combustion (%)	29.8	—	28.9	—
Char to combustion chamber (wt%) per dry biomass	—	13.2	—	11.9
SNG output (kW)	333.8	356.8	334.5	368.5
Auxiliary power demand (kW)	9.4	10.3	9.4	9.7
Heat above 60 °C (kW)	97.6	122.8	98.3	110.7

of the heat output as a product leads to an overall efficiency of 81.6% in process 1. The performance is marginally influenced by steam integration but is strongly enhanced by char integration. In process 2 and process 4, an overall efficiency of 90.7% and 91.0%, respectively, is feasible.

If the conversion of tars in the methanation reactor has a negative impact on the catalyst, tars need to be removed in the gas cleaning unit. The decrease of the efficiency is then dependent on the tar concentration and the usage of the tar waste stream. Preliminary estimations result in a possible decrease of the conversion efficiency of 2–5 percent points, but a detailed calculation is not given here.

A simple comparison of the process performance with other studies is not always possible, as the calculated efficiency depends on its definition (for example, chemical conversion, energy, and exergy) and the chosen boundary conditions (for example, biomass moisture content, biomass pretreatment, and SNG compression). However, when only the chemical conversion efficiency is compared, the system performance reported here is within the range that is reported in literature. Gassner and Marechal [5] analyzed the SNG production in a larger scale (20 MW<sub>th</sub>) and calculated a conversion efficiency between 67.2% and 73.8%, depending on the gasifier type (indirect steam gasifier or oxygen-blown circulating fluidized bed gasifier) and process conditions. Zwart *et al.* [6] calculated a conversion efficiency of only 68.5%, which is due to the gas cooling and tar removal after the gasification and the fact that the overall system is coupled with a steam cycle and power produced in addition to SNG. Therefore, the focus of the study was on the overall system efficiency. Van der Meijden *et al.* [7] calculated an efficiency of 70.3% for the large-scale SNG production based on an atmospheric indirect gasifier and a compression prior to the methanation.

The efficiency of process 1 is very low compared with the literature data. If the removal of tar after the gasification might be necessary, the performance will further decrease. The simulation shows the disadvantage of a small-scale system that is not integrated. However, the integration of the two fluidized beds via a char transfer enables a very high efficiency compared with larger-scale systems.

## 5.2. Heat output

The different processes allow different amounts of heat to be used by a heat consumer. The heat quantities for the four processes are summarized in Table V. The heat

released is mainly dependent on the integration of reformer and combustor and determines the overall efficiency. If all heat sources are used, process 2 reaches the same overall efficiency as process 4 and requires no steam integration.

If the production of SNG is simulated on a larger scale, the heat output is used in a steam cycle [7] for additional power production. On the small scale, the production of electricity is not considered and the power demand is taken from the electricity grid.

## 5.3. Synthetic natural gas quality

Because of the identical gas processing systems, there are only marginal differences in the SNG composition produced in the four processes. Table VI shows the SNG composition and the gas quality parameters of process 4.

The gas mainly consists of methane, hydrogen, and carbon dioxide. A small amount of nitrogen comes from the feeding system of biomass to the gasifier. In contrast to larger systems, the feeding with air is considered on the small scale. The storage and usage of the off-gas of the PSA that mainly consists of CO<sub>2</sub> is not considered as this would additionally complicate the small-scale process.

Chlorine and sulfur compounds are not present in the SNG because these elements are removed prior to methanation.

The Wobbe index evaluates the applicability of different fuel gases. Gases with the same Wobbe index result in an identical heat load of a burner at identical die pressure. For the injection into the German gas grid, the Wobbe index has to be in the range 46.1–56.5 MJ Nm<sup>-3</sup>, and the maximal concentrations of CO<sub>2</sub> and H<sub>2</sub> are 6% and 5% (mole fraction), respectively [47]. Hence, the SNG produced in this small-scale process meets the requirements for injection into the natural gas grid.

**Table VI.** Synthetic natural gas composition (mole fraction) and gas properties of process 4 at the point of injection into the natural gas grid.

Parameter	Value
CH <sub>4</sub>	88.7%
CO <sub>2</sub>	3.3%
H <sub>2</sub>	4.8%
N <sub>2</sub>	3.2%
Wobbe index	47.0 MJ Nm <sup>-3</sup>
Relative density	0.57

## 6. CONCLUSIONS

A small-scale process that allows the production of SNG from biomass with a thermal biomass input of 500 kW has been designed and simulated in Aspen Plus. As expected, the higher the integration of the process, the higher the efficiency. A high overall efficiency of more than 90% that includes usable heat output is achievable by integrating reformer and combustor, that is, by feeding char to the combustion reactor. The fully integrated process reaches a net efficiency of 68.9% and an overall efficiency of 91.0%. The SNG quality in all processes meets the requirements for injection into the natural gas grid.

The process simulation shows that the performance of the small-scale system approaches the efficiencies of larger systems that are reported in literature, but some requirements have to be fulfilled. The gasifier has to be operated at an increased pressure to avoid a compression prior to the methanation reactor, the process is operated without the removal of tars that are converted in the methanation reactor, and a char integration between the two fluidized beds is required. Any process integration in a small-scale system is a challenging task; however, the BioHPR technology has demonstrated the char integration on a scale below 1 MW.

Synthetic natural gas production offers advantages to direct biomass utilization for electricity or CHP. The SNG can be used in a gas turbine combined cycle with electrical efficiencies of up to 60% [48]. Hence, a biomass-to-electricity efficiency of up to 41%, which is within the range of larger-scale state-of-the-art coal power plants, is technically feasible. The focus of biomass usage could also be on overall efficiency including heat utilization. In this case, SNG can be used for CHP production. Modern CHP units realize an electrical efficiency of 41.7% and an overall efficiency of 90% [46]. When several small-scale SNG plants feed gas to the natural gas grid and the gas is consumed by one or several CHP units, the concept offers an overall CHP efficiency of up to 81%. The biomass-to-electricity efficiency, in this case, is up to 28%. Both values are in the range of multi-megawatt biomass CHP plants. However, the small-scale production of SNG in a first step has two advantages. Firstly, only a small amount of heat (approximately 100 kW) is released at the location of SNG production, making it easy to find an appropriate heat consumer (e.g., apartment house, small industry building, and school building). Secondly, the usage of the natural gas infrastructure as temporary storage enables the heat production in a CHP to be adapted to the present needs of the heat consumer.

## ACKNOWLEDGEMENTS

The authors are grateful to Markus Stemann and Prof. Dr.-Ing. Dietmar Hein (hs energieanlagen GmbH, Freising, Germany) for their helpful discussion and their information provided in this field. This work was done within the framework of the TUM Graduate School.

## REFERENCES

1. European Union. Directive on the promotion of the use of energy from renewable sources. 2009/28/EC, 2009.
2. Rönsch S, Dreher M, Vogel A, Kaltschmitt M. Synthetic natural gas from solid biofuels—a technical analysis. *VGB Powertech* 2008; **88**(5):110–116.
3. Ramesohl S, Arnold K. *Analyse und Bewertung der Nutzungsmöglichkeiten von Biomasse*. Wuppertal Institut: Wuppertal, 2006.
4. Duret A, Friedli C, Maréchal F. Process design of synthetic natural gas (SNG) production using wood gasification. *Journal of Cleaner Production* 2005; **13**(15):1434–1446.
5. Gassner M, Maréchal F. Thermo-economic process model for thermochemical production of synthetic natural gas (SNG) from lignocellulosic biomass. *Biomass and Bioenergy* 2009; **33**(11):1587–1604.
6. Zwart R, Boerrigter H, Deurwaarder E, van der Meijden C, van Paasen S. Production of synthetic natural gas (SNG) from biomass. ECN-E-06-018. ECN, 2006.
7. van der Meijden CM, Veringa HJ, Rabou LPLM. The production of synthetic natural gas (SNG): a comparison of three wood gasification systems for energy balance and overall efficiency. *Biomass and Bioenergy* 2010; **34**(3):302–311.
8. Heyne S, Thunman H, Harvey S. Integration aspects for synthetic natural gas production from biomass based on a novel indirect gasification concept. In: 11th Conference on Process Integration, Modelling and Optimisation for Energy Saving and Pollution Reduction, 2008.
9. Heyne S, Seemann MC, Harvey S. Integration study for alternative methanation technologies for the production of synthetic natural gas from gasified biomass. *Chemical Engineering Transactions* 2010; **21**. DOI: 10.3303/CET1021069.
10. Heyne S, Thunman H, Harvey S. Extending existing combined heat and power plants for synthetic natural gas production. *International Journal of Energy Research* 2012; **36**(5):670–681.
11. Jurascik M, Sues A, Ptasinski KJ. Optimization of biomass to-synthetic natural gas conversion technology based on exergy analysis. In *Proceedings of the 16th European Biomass Conference & Exhibition*. 2008.
12. Juraščík M, Sues A, Ptasinski KJ. Exergy analysis of synthetic natural gas production method from biomass. ECOS 2008 21st International Conference, on Efficiency, Cost, Optimization, Simulation and Environmental Impact of Energy Systems. *Energy* 2010; **35**(2):880–888.
13. Rehling B, Hofbauer H, Rauch R, Aichernig C. BioSNG—process simulation and comparison with first results from a 1-MW demonstration plant. *Biomass Conversion and Biorefinery* 2011; **1**(2):111–119.

14. Seemann MC, Schildhauer TJ, Biollaz SMA. Fluidized bed methanation of wood-derived producer gas for the production of synthetic natural gas. *Industrial & Engineering Chemistry Research* 2010; **49**(15):7034–7038.
15. Gunnarsson I. The GoBiGas Project. Efficient transfer of biomass to bio-SNG of high quality. In: SGC International Seminar on Gasification, 2011.
16. Möller BF. Gasification development at E.ON. In: SGC International Seminar on Gasification, 2010.
17. Wei L, To SDF, Pordesimo L, Batchelor W. Evaluation of micro-scale electricity generation cost using biomass-derived synthetic gas through modeling. *International Journal of Energy Research* 2011; **35**(11):989–1003.
18. Metz T. Allotherme Vergasung von Biomasse in indirekt beheizten Wirbelschichten. Dissertation, Technische Universität München, 2007.
19. Karl J. Distributed generation of substitute natural gas from biomass. In *Proceedings of the 16th European Biomass Conference & Exhibition*. 2008.
20. Karellas S, Karl J, Kakaras E. An innovative biomass gasification process and its coupling with microturbine and fuel cell systems. 19th International Conference on Efficiency, Cost, Optimization, Simulation and Environmental Impact of Energy Systems ECOS 2006. *Energy* 2008; **33**(2):284–291.
21. Gómez-Barea A, Leckner B. Modeling of biomass gasification in fluidized bed. *Progress in Energy and Combustion Science* 2010; **36**(4):444–509.
22. Puig-Arnabat M, Bruno JC, Coronas A. Review and analysis of biomass gasification models. *Renewable and Sustainable Energy Reviews* 2010; **14**(9):2841–2851.
23. Buragohain B, Mahanta P, Moholkar VS. Performance correlations for biomass gasifiers using semi-equilibrium non-stoichiometric thermodynamic models. *International Journal of Energy Research* 2012; **36**(5):590–618.
24. Abuadala A, Dincer I. A review on biomass-based hydrogen production and potential applications. *International Journal of Energy Research* 2012; **36**(4):415–455.
25. Mathieu P, Dubuisson R. Performance analysis of a biomass gasifier. *Energy Conversion and Management* 2002; **43**(9–12):1291–1299.
26. Nikoo MB, Mahinpey N. Simulation of biomass gasification in fluidized bed reactor using ASPEN PLUS. *Biomass and Bioenergy* 2008; **32**(12):1245–1254.
27. Vera D, Jurado F, Panopoulos KD, Grammelis P. Modelling of biomass gasifier and microturbine for the olive oil industry. *International Journal of Energy Research* 2012; **36**(3):355–367.
28. Shen L, Gao Y, Xiao J. Simulation of hydrogen production from biomass gasification in interconnected fluidized beds. *Biomass and Bioenergy* 2008; **32**(2):120–127.
29. Panopoulos KD, Fryda LE, Karl J, Poulou S, Kakaras E. High temperature solid oxide fuel cell integrated with novel allothermal biomass gasification: part i: modelling and feasibility study. *Journal of Power Sources* 2006; **159**(1):570–585.
30. Hofbauer H, Rauch R, Fürnsinn S, Aichernig C. Energiezentrale Güssing. Energiezentrale zur Umwandlung von biogenen Roh- und Reststoffen einer Region in Wärme, Strom, BioSNG und flüssige Kraftstoffe, Vienna, 2006.
31. Seglin L. *Methanation of Synthesis Gas*, vol. **146**. American Chemical Society: Washington, D. C, 1975.
32. Mozaffarian M, Zwart R, Boerrigter H, Deurwaarder E. Biomass and waste-related SNG production technologies. In *Proceedings of the 2nd World Conference and Technology Exhibition on Biomass for Energy, Industry and Climate Protection*. 2004.
33. Boerrigter H, van Paasen S, Bergman P, Könemann J, Emmen R. Tar removal from biomass product gas. development and optimisation of the OLGA tar removal technology. In *Proceedings of the 14th European Biomass Conference & Exhibition*. 2005.
34. Stevens DJ. Hot Gas Conditioning: Recent Progress with Larger-Scale Biomass Gasification Systems, NREL/SR-510-29952. National Renewable Energy Laboratory, 2001.
35. Dayton D. A Review of the Literature on Catalytic Biomass Tar Destruction, NREL/TP-510-32815. National Renewable Energy Laboratory, 2002.
36. Nacken M, Ma L, Engelen K, Heidenreich S, Baron GV. Development of a tar reforming catalyst for integration in a ceramic filter element and use in hot gas cleaning. *Industrial and Engineering Chemistry Research* 2007; **46**(7):1945–1951.
37. Pfeifer C, Hofbauer H. Development of catalytic tar decomposition downstream from a dual fluidized bed biomass steam gasifier. Gas cleaning at high temperature: papers presented at the 6th International Symposium on Gas Cleaning at High Temperature, Osaka, Japan 20–22 October 2005. *Powder Technology* 2008; **180**(1–2):9–16.
38. Seemann M, Biollaz S, Stucki S. Thermo-chemical analysis of the production of SNG from wood. In *Proceedings of the 15th European Biomass Conference & Exhibition*. 2007.
39. Newby RA, Smeltzer EE, Lippert TE, Slimane RB. Novel Gas Cleaning/Conditioning for Integrated Gasification Combined Cycle, DE-AC26-99FT40674. Siemens Westinghouse Power Corporation, 2001.
40. van Paasen S, Cieplik M, Phokawat N. Gasification of Non-woody Biomass, ECN-C-06-032. ECN, 2006.
41. Fürnsinn S, Hofbauer H. Synthetische Kraftstoffe aus Biomasse: Technik, Entwicklungen, Perspektiven. *Chemie Ingenieur Technik* 2007; **79**(5):579–590.

42. Panek JM, Grasser J. Practical Experience Gained During the First Twenty Years of Operation of the Great Plains Gasification Plant and Implications for Future Projects. US Department of Energy, 2006.
43. FactSage 5.5. Thermfact and GTT-Technologies, 2009.
44. Seemann MC, Schildhauer TJ, Biollaz SMA, Stucki S, Wokaun A. The regenerative effect of catalyst fluidization under methanation conditions. *Applied Catalysis A: General* 2006; **313**(1):14–21.
45. Kopyscinski J, Schildhauer TJ, Biollaz SMA. Production of synthetic natural gas (SNG) from coal and dry biomass—A technology review from 1950 to 2009. *Fuel* 2010; **89**(8):1763–1783.
46. Urban W, Lohmann H, Girod K. Technologien und Kosten der Biogasaufbereitung und Einspeisung in das Erdgasnetz. Ergebniss der Markterhebung 2007–2008. Fraunhofer UMSICHT, Oberhausen, 2009.
47. DVGW. Technische Regel Arbeitsblatt G 262 - Nutzung von Gasen aus regenerativen Quellen in der öffentlichen Gasversorgung(G262), 2002.
48. Fischer R, Ratliff P, Fischer W. SGT5-8000 H - Product Validation at Irsching 4 Test Center. In *Proceedings of POWER-GEN Asia*. 2008.